RESEARCH PAPER

Formulation and in Vitro Evaluation of Imiquimod-Loaded Zinc Oxide–Mesoporous Silica Hybrid Nanoparticles for Skin Cancer Therapy

Shubham Solanki[a*], Mangesh Kulkarni[b], Samir Atara[c]

[a*] Ph.D. Scholar, Department of Pharmaceutics, School of Pharmacy, RK University, Rajkot - 360020, Gujarat, India. (Corresponding Author) Contact No: +91-8200527071, Email: shubham.p.solanki@gmail.com

[b] Assistant Professor, Department of Pharmaceutics, Gandhinagar Institute of Pharmacy, Gandhinagar University.

[c] Professor, Department of Pharmaceutics, School of Pharmacy, RK University, Rajkot - 360020, Gujarat, India.

Received: 20th Feb, 2026 | **Revised:** 4th Mar, 2026 | **Accepted:** 25th Mar, 2026 | **Available Online:** 10th Apr, 2026

ABSTRACT

Background: Basal cell carcinoma represents the most common type of non-melanoma skin cancer, frequently addressed with topical immunomodulators like Imiquimod. Nonetheless, traditional topical formulations frequently encounter challenges such as inadequate skin penetration, rapid drug release, and significant local irritation, which can hinder patient adherence and overall therapeutic effectiveness.

Methods: This study focused on the development and assessment of Imiquimod-loaded zinc oxide functionalized mesoporous silica nanoparticles as an innovative topical nanocarrier system for enhanced management of Basal cell carcinoma. Mesoporous silica nanoparticles were created through a surfactant-templated sol–gel approach and later modified with zinc oxide to improve drug affinity and provide extra dermatological advantages. Imiquimod was incorporated utilizing a solvent adsorption method, and the optimized zinc oxide-mesoporous silica nanoparticles were integrated into a biocompatible topical gel.

Results: The characterization of the formulation included assessments of particle size, drug entrapment efficiency, loading capacity, and in-vitro release behavior, all conducted using a validated high performance liquid chromatography. The safety of the formulation was evaluated through the assessment of cytotoxicity in B16-F10 melanoma cells. Zinc oxide-mesoporous silica nanoparticles exhibited a notably enhanced drug entrapment rate of approximately 94% and a sustained diffusion-controlled release, surpassing that of plain mesoporous silica nanoparticles. The topical gel demonstrated a controlled drug release for up to 72 hours and showed reduced cytotoxicity compared to free Imiquimod, suggesting enhanced tolerability. The release kinetics adhered to the Higuchi diffusion model, validating the transport of the drug through a porous matrix.

Conclusion: The developed zinc oxide-mesoporous silica nanoparticles-based gel presents a compelling approach for improving the safety, efficacy, and patient acceptability of topical Imiquimod therapy in the treatment of basal cell carcinoma.

Keywords: Basal Cell Carcinoma, Imiquimod, Mesoporous Silica Nanoparticles, Zinc Oxide Functionalization, Topical Nanocarrier System.

How to cite this article: Solanki S, Kulkarni M, Atara S. Formulation and in Vitro Evaluation of Imiquimod-Loaded Zinc Oxide–Mesoporous Silica Hybrid Nanoparticles for Skin Cancer Therapy. Int J Drug Deliv Technol. 2026;16(32s):52-65. DOI: 10.25258/ijddt.16.32s.7

Source of support: Nil.

Conflict of interest: The authors declare no conflict of interest.

1 INTRODUCTION

Basal cell carcinoma (BCC) represents the most commonly identified skin cancer, constituting approximately 70-80% of non-melanoma skin cancer cases globally. This condition arises from the basal layer of the epidermis and typically presents as a slowly enlarging, pearly or flesh-toned nodule in areas frequently exposed to sunlight, including the face, scalp, or neck. While BCC infrequently metastasizes, its advancing local invasion can lead to considerable tissue damage, functional impairment, and cosmetic disfigurement if not addressed promptly. Ultraviolet radiation continues to be the leading cause of risk, with heightened outdoor exposure leading to a persistent increase in global incidence rates[1].

The National Comprehensive Cancer Network (NCCN) Guidelines for Basal Cell Skin Cancer delineate three distinct risk categories: low-risk BCC, high-risk BCC, and advanced BCC. The high-risk characteristics include: placement on the head, neck, hands, feet, pretibial, and anogenital regions (regardless of size); placement on the trunk or extremities with a tumor size of 2 cm or larger; indistinct clinical borders; recurrent basal cell carcinoma; patients with immune suppression; a history of previous radiotherapy; and high-risk pathological features (as detailed below). When any of the high-risk features mentioned above are observed, the lesion is classified as high-risk BCC; conversely, in all other instances, it is categorized as low-risk BCC. The third category encompasses advanced BCC, which includes both laBCC and mBCC. For each of these categories, distinct treatment options are necessary[2].

The development of cancer cannot be attributed to a singular cause. Indeed, a variety of internal and external factors play a role in the onset of cancer[3]. Internal factors encompass mutations in genes, genetic disorders, and hormone imbalances, while external factors involve exposure to radiation, malnutrition, infectious agents, tobacco use, and more[4]. Approximately 90% of deaths associated with cancer result from the spread of tumors, a process known as metastasis. A hereditary gene defect accounts for merely 5-10% of all cancer cases. Although all tumors arise from a combination of mutations, these mutations result from interactions with environmental factors and carcinogens[5].

The primary characteristics of cancer are presented in **Figure 1**. The image depicts the defining characteristics of cancer, encapsulating the essential biological traits that normal cells gain as they evolve into malignant tumor cells. At the core lies a mass of cancer cells, encircled by a network of interconnected processes that together propel tumor initiation, progression, and metastasis. The characteristics outlined here elucidate the reasons behind the unchecked proliferation of cancer cells, their defiance of regulatory controls, and their capacity to infiltrate adjacent tissues.

A key characteristic observed is the persistent activation of proliferative signaling, wherein cancer cells incessantly engage growth pathways, resulting in unregulated replication. This is intricately connected to a lack of responsiveness to signals that inhibit growth, enabling tumor cells to bypass standard regulatory checkpoints. In addition, cancer cells demonstrate a remarkable ability to evade apoptosis, allowing them to persist even in the face of genetic damage or adverse conditions. Genomic instability significantly enhances cancer progression by elevating mutation rates, thereby fostering tumor heterogeneity and adaptability.

The image further emphasizes the altered cellular energetics, illustrating the ways in which cancer cells modify their metabolism to satisfy elevated energy and biosynthetic requirements. The ability of malignant cells to evade immune destruction enables them to escape detection and elimination by the immune system, thereby ensuring their continued existence. Furthermore, tumors develop the capability to stimulate angiogenesis, leading to the formation of new blood vessels that provide the oxygen and nutrients essential for continued growth. Ultimately, advanced cancers acquire the ability to invade and metastasize, allowing cells to separate, move, and establish themselves in distant organs. The portrayal of unregulated replication and the avoidance of signals for cell destruction highlights the disabling of tumor suppressor pathways throughout the process of carcinogenesis. This image collectively illustrates that cancer arises not from a singular defect, but from the accumulation of various interconnected biological changes, offering a conceptual framework for comprehending tumor biology and pinpointing potential therapeutic targets.

A variety of therapeutic approaches are presently utilized for the management of BCC, encompassing excision, cryotherapy, photodynamic therapy, curettage and desiccation, laser ablation, and topical chemotherapy. Among topical medications, Imiquimod has become a significant non-invasive immunomodulatory treatment. This mechanism involves the activation of toll-like receptor-7 (TLR-7), which leads to the stimulation of cytokine release, enhancement of antigen presentation, and the induction of cell-mediated antitumor immune responses. While conventional topical administration of Imiquimod offers therapeutic benefits, it is accompanied by limitations including local irritation, burning, erythema, dryness, and inadequate dermal penetration, which can result in inconsistent therapeutic outcomes. The identified limitations underscore the pressing requirement for a more effective delivery system that optimizes drug localization, minimizes adverse effects, and ensures prolonged release at the intended site[6].

Topical drug delivery systems utilizing nanotechnology have demonstrated significant potential in overcoming these challenges. Among these materials, mesoporous silica nanoparticles (MSNs) have attracted significant interest owing to their adjustable pore structure, extensive surface area, substantial drug loading capacity, customizable surface chemistry, and favorable biocompatibility. MSNs, especially MCM-41, exhibit a honeycomb-like structure characterized by uniformly ordered cylindrical pores, which facilitate stable drug encapsulation and regulated diffusion into the skin layers. Their readily adaptable surface facilitates the attachment of therapeutic or bioactive molecules, enhancing targeted delivery and pharmacodynamic effectiveness[7,8].

Moreover, the incorporation of zinc oxide (ZnO) into MSNs enhances their therapeutic potential. ZnO demonstrates properties that promote wound healing, reduce inflammation, modulate immune responses, combat microbial activity, and block UV radiation, making it advantageous for applications in dermatology[9]. This also facilitates epithelial regeneration and alleviates irritation, potentially mitigating the negative effects linked to topical Imiquimod treatment. Consequently, the combination of ZnO with MSNs offers a synergistic strategy that merges substantial drug loading and regulated release with advantages for skin protection[10].

This study focuses on the formulation and assessment of Imiquimod-loaded ZnO-functionalized mesoporous silica nanoparticles (ZnO-MSNs) in a topical gel format. The research highlights the importance of refining drug loading parameters, conducting physicochemical characterization, evaluating in-vitro diffusion, and assessing cytotoxicity. The primary aim is to create an advanced topical delivery system that boosts the therapeutic effectiveness of Imiquimod, reduces irritation, and enhances overall treatment results for BCC[11].

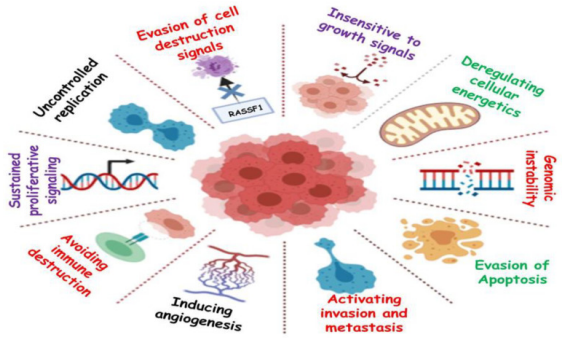

Figure 1 Pictorial Representation of Hallmarks of Cancer (The image is adopted under CC 4.0[11] (https://doi.org/10.3390/cancers13184570)

2 MATERIALS AND METHODS

2.1 Materials

Imiquimod was selected as the model therapeutic agent for nanoparticle loading. Tetraethyl orthosilicate (TEOS) and cetyltrimethylammonium bromide (CTAB) served as precursors for mesoporous silica synthesis, while zinc nitrate was used for zinc oxide functionalization. Triethylamine, orthophosphoric acid, acetonitrile, and analytical/HPLC-grade methanol were utilized for drug loading and analytical studies. All chemicals were procured from authenticated suppliers and used without further purification. Distilled water was employed in all experimental procedures. The materials and chemicals used for the development, synthesis, and functionalization are mentioned in **Table *1*.**

Table 1 List of Procured materials and chemicals

Sr. No.	Materials/Chemicals	Obtained from
1	Imiquimod	Dr. Reddy's Laboratories
2	Tetraethyl orthosilicate (TEOS)	SD Fine Chemicals
3	Cetyltrimethylammonium bromide (CTAB)	SD Fine Chemicals
4	Zinc Nitrate	SD Fine Chemicals
5	Triethylamine	SD Fine Chemicals
6	Orthophosphoric acid	SD Fine Chemicals
7	Acetonitrile	SD Fine Chemicals
8	Methanol	SD Fine Chemicals
9	Distilled water	Rankem Chemicals

2.2 Synthesis of Mesoporous silica nanoparticles:

The chemistry of silica through sol-gel processes has historically concentrated on adjusting the size, shape, and distribution of silica particles. This focus is due to the straightforward nature of the operation, the mild conditions involved, and the ability to control the hydrolysis and condensation of silicon alkoxide, especially tetraethyl orthosilicate (TEOS). The synthesis of mesoporous silica like MCM-41 requires the inclusion of CTAB as a structure-directing agent, along with ammonia to enhance the hydrolysis and condensation of TEOS. The self-assembly of silanol monomers in conjunction with the CTAB surfactant

leads to the creation of colloidal mesoporous silica exhibiting a variety of architectures. A prominent instance is the creation of hollow mesoporous silica spheres, characterized by their structured pore size, ample cavity, elevated surface area, and diverse applications in drug storage and release, catalysis, adsorption, and separation, among others[12,13].

Recent investigations have demonstrated that silica particles synthesized through the sol–gel method display intrinsic inhomogeneity. For example, Haes and colleagues described a targeted etching approach utilizing hydrofluoric acid (HF) to create hollow silica spheres. The initial design involved organic–inorganic silica particles featuring a core-shelled structure. The outer layer consisted of a pure silica framework derived from hydrolyzed TEOS, whereas the sacrificial layer was made up of organic silica resulting from the co-condensation of TEOS and N-[3-(trimethoxysilyl)propyl]ethylenediamine (TSD). The less compact structures of the organic silica frameworks render them vulnerable to hydrofluoric acid (HF) attack. It is clear that the sol–gel method provides the benefit of producing hollow spheres characterized by a tight size distribution and robust structures. For instance, integrating the sol–gel technique with the emulsion method improves emulsion stability while also facilitating the hydrolysis and condensation of TEOS in the synthesis of hollow MCM-41 spheres[14,15].

MSNs were synthesized via a surfactant-templated sol-gel process. CTAB was dissolved and allowed to self-assemble into a micellar template under alkaline aqueous conditions. TEOS was subsequently added dropwise, followed by controlled stirring to facilitate hydrolysis and condensation around the surfactant micelles. The solid product was filtered, washed thoroughly, and calcined at an elevated temperature to remove CTAB, yielding a highly porous MSN framework with uniformly distributed cylindrical pores.

2.3 Analytical Method Development for Imiquimod (HPLC Method)

The analytical techniques utilized for quantifying drugs in in vitro skin penetration studies must be precise, as these samples are often tainted with endogenous skin compounds, which include a significant variety of UV-absorbing nucleotides and nucleosides. Furthermore, it is essential for these methods to demonstrate sufficient sensitivity, given the limited volume of the sample (receptor medium) and the small dimensions of horizontal skin layers, including the stratum corneum (SC), viable epidermis, and dermis acquired from Franz diffusion cells.

A method utilizing reverse phase liquid chromatography (RP-HPLC) has been validated for the quantification of Imiquimod. Separation was accomplished using a cosmosil C18 column (250 mm × 4.6 mm I.D; particle size 5 µm). The mobile phase consisted of a pH 4.6 phosphate buffer and acetonitrile in a 20:80 v/v ratio, with a flow rate of 0.8 mL/min. The column temperature was kept at 25°C. UV detection was conducted at 244 nm, with a total run time of 10 minutes. The approach is straightforward, efficient, and targeted. The method for imiquimod demonstrates linearity across a range of 5 ng/mL to 600 ng/mL, achieving a correlation coefficient of 0.992. The precision of the method for assay determination was found to be below 2.0% Relative Standard Deviation (RSD). The method facilitates an accurate, precise, and swift analysis of imiquimod.

A standard calibration curve of Imiquimod was prepared in methanol, and the linearity was confirmed within an analytical concentration range based on the obtained absorbance values.

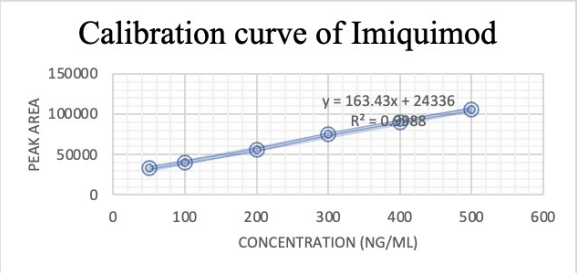

Figure 2 Calibration curve of Imiquimod in pH 4.6 phosphate buffer and acetonitrile in a 20:80 v/v ratio

2.4 Synthesis of Mesoporous Silica Nanoparticles (MCM-41)

Mesoporous silica nanoparticles (MSNs) were synthesized through a traditional surfactant-templated sol-gel approach aimed at obtaining a well-ordered porous structure. In summary, cetyltrimethylammonium bromide (CTAB) was dissolved in deionized water under alkaline conditions, which were typically adjusted using an appropriate base, while the solution was kept at a controlled temperature with continuous stirring. In these circumstances, CTAB molecules exhibited spontaneous self-assembly, resulting in the formation of well-defined micellar structures that served as structure-directing templates for the creation of mesopores. Following this, tetraethyl orthosilicate (TEOS) was added dropwise to the reaction mixture,

serving as the silica precursor. The gradual incorporation of TEOS, along with regulated stirring, facilitated consistent hydrolysis and polycondensation processes, resulting in the gradual formation of a silica network encasing the CTAB micelles[16].

Upon finishing the sol-gel reaction, the solid precipitate was gathered through filtration and thoroughly washed with deionized water and/or ethanol to eliminate any unreacted species and loosely attached surfactant. The material obtained was subsequently subjected to calcination at a high temperature for a specified period to ensure the complete removal of the organic surfactant template. The thermal treatment resulted in a strong mesoporous silica framework distinguished by an elevated specific surface area, a narrow pore size distribution, and uniformly aligned cylindrical mesopores, rendering the synthesized MSNs appropriate for cutting-edge applications including drug delivery, adsorption, and catalysis[17].The **Figure 3** clearly depicts the particle size distribution (PSD) and morphology of synthesized MSNs.

Figure 3 The illustration presents the results of dynamic light scattering (DLS) for a dispersion of nanoparticles. The analysis reveals a Z-average particle size of around 318 nm, reflecting the hydrodynamic diameter of the suspended particles. The polydispersity index (PDI) of 0.201 indicates a relatively narrow size distribution and an acceptable level of uniformity within the sample. The intercept value of 0.930, along with the classification of the result quality as “Good,” suggests a dependable correlation and consistent measurement stability.

The intensity size distribution shows a prominent peak at approximately 319 nm, contributing 100% to the intensity. This indicates that the formulation is predominantly monodisperse, with no notable aggregation or presence of secondary particle populations. The standard deviation indicates a moderate level of variability in relation to the average size. The DLS profile demonstrates a well-dispersed nanoparticulate system characterized by uniform particle size, making it appropriate for subsequent physicochemical characterization or application studies.

Figure 3 Particle size distribution and morphology of synthesized MSNs

2.5 Functionalization of MSNs with Zinc Oxide

To improve drug adsorption and offer further therapeutic benefits, MSNs were modified with zinc oxide (ZnO). A precise concentration of zinc nitrate solution was applied to MSNs, subsequently adjusting the pH to initiate the controlled precipitation of zinc hydroxide. The precipitate underwent drying and calcination to transform zinc hydroxide into ZnO, resulting in the formation of ZnO-functionalized MSNs (ZnO-MSNs). The elemental composition of Zn, Si, and O within the nanostructure was validated using energy dispersive spectroscopy (EDS)[18].

The incorporation of ZnO into MCM-41 was achieved through a post-synthesis approach. In summary, 0.1 g of zinc chloride (ZnCl2) was dissolved in deionized water, and 0.5 g of MCM-41 was added and stirred for 6 hours. The pH was adjusted to 8.0 by the addition of a 0.1 M sodium hydroxide solution. The mixture was subsequently aged for 10 hours following 6 hours of stirring. The mixture was filtered, thoroughly rinsed with deionized water multiple times, dried at 80°C overnight, and subsequently calcined at 550°C for 2 hours to yield ZnO-loaded MCM-41 (ZnO-MSNs)[19].

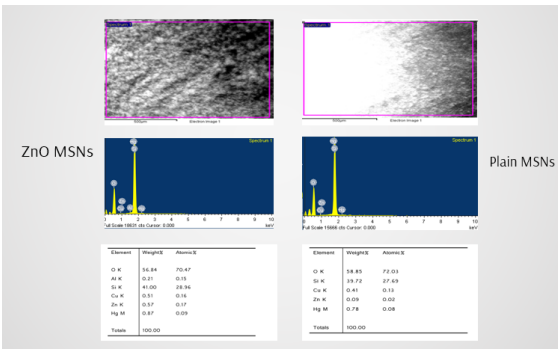

Figure 4 EDS spectrum confirming presence of Zn, Si, and O

The **Figure 4** mentions a comparative analysis using scanning electron microscopy (SEM) and energy-dispersive X-ray spectroscopy (EDS) of ZnO-loaded mesoporous silica nanoparticles (ZnO MSNs)

alongside plain mesoporous silica nanoparticles (plain MSNs), emphasizing the morphological and elemental distinctions between the two systems[20].

The SEM micrographs (upper panel) demonstrate that both formulations display a fairly consistent and aggregated nanoparticulate morphology, typical of mesoporous silica–based materials. The surface texture of ZnO MSNs is observed to be somewhat rougher than that of plain MSNs, a phenomenon that can be linked to the effective incorporation or deposition of ZnO within or onto the mesoporous silica framework. This morphological change offers qualitative proof of surface modification while maintaining the integrity of the silica matrix structure.

The accompanying EDS spectra (lower panel) provide additional confirmation of the compositional differences observed between the samples. The spectrum for plain MSNs primarily exhibits robust signals for oxygen (O) and silicon (Si), aligning with the silica backbone. Additionally, there are minor traces of aluminum (Al), sulfur (S), copper (Cu), and magnesium (Mg), which could originate from synthesis reagents, substrates, or instrumental background. Conversely, the ZnO MSNs display a distinct zinc (Zn) peak, which validates the effective integration of ZnO within the mesoporous silica framework. The elevated weight and atomic percentages of Zn in the ZnO MSN sample confirm its presence significantly above mere trace contamination levels[21].

The comprehensive SEM-EDS analysis reveals that the integration of ZnO maintains the essential morphology of MSNs while successfully incorporating zinc species into the system. This validates the successful creation of ZnO-loaded MSNs, highlighting their promising applications in areas like antimicrobial delivery, catalytic systems, or sophisticated pharmaceutical nanocarriers[22].

2.6 Drug Loading of Imiquimod

Imiquimod was integrated into plain MSNs and ZnO-MSNs through a solvent adsorption technique. Different organic solvents and drug-to-carrier ratios were examined to enhance loading efficiency. Following incubation, the unencapsulated drug was isolated through centrifugation, and the quantity of the entrapped drug was measured utilizing the validated HPLC technique[23]. The calculations for entrapment efficiency (% EE) and loading capacity (% LC) were performed using the equations outlined below:

$$Loading\ Capacity\ (LC) = \left(\frac{\text{Weight of drug incorporated}}{\text{Weight of drug-loaded carrier}}\right) \times 100\%$$

$$Entrapment\ Efficiency = \left(\frac{\text{Weight of drug incorporated}}{\text{Weight of drug added}}\right) \times 100\%$$

Table 2 Comparison of % EE and % LC of plain MSNs and ZnO-MSNs

Sr. No	Type of MSNs	DRUG:MSN Ratio	SOLVENTS	DRUG CONC.	%Entrapment ± SD	%Loading ± SD capacity
1	Plain MSNs	1:1	Acetate buffer (pH 4.0) and Methanol (3:7)	1 mg/ml	81.88 ± 3.489	45.01 ± 1.05
2	ZnO-MSNs	1:1	Acetate buffer (pH 4.0) and Methanol (3:7)	1 mg/ml	93.94 ± 3.81	48.42 ± 1.02

2.7 Preparation of Topical Gel

The optimized ZnO-MSNs containing Imiquimod were incorporated into a gel base utilizing a hydrated polymer. The gel underwent homogenization to achieve a consistent distribution of nanoparticles. The ultimate formulation underwent assessment for its appearance, pH, viscosity, spreadability, homogeneity, and uniformity of drug content[24].

The formulation of the topical gel containing imiquimod was developed utilizing a standard polymeric gel base, aimed at achieving optimal drug distribution, stability, and suitability for skin application. To begin, an appropriate gelling agent, like Carbopol 934/940, HPMC, or another approved polymer, was precisely measured and slowly

incorporated into purified water while stirring continuously to avoid the formation of lumps. The dispersion was permitted to fully hydrate for a specified duration to ensure consistent swelling of the polymer chains[25].

Imiquimod, an immunomodulatory drug with limited solubility in water, was either dissolved individually or uniformly dispersed within a suitable solvent system (including ethanol, propylene glycol, or a combination of these), which also served as a penetration enhancer. This phase enhanced the solubilization of the drug and promoted its uniform integration into the gel matrix. The drug solution was subsequently introduced gradually into the hydrated polymer dispersion while maintaining continuous stirring to achieve a homogeneous drug-loaded gel[26].

Following this, additional excipients including humectants like glycerin or propylene glycol, preservatives such as methyl paraben or propyl paraben, and permeation enhancers were integrated according to the formulation specifications. The formulation's pH was meticulously adjusted with a neutralizing agent, like triethanolamine or sodium hydroxide, to achieve a skin-compatible pH, generally within the range of 5.5–6.5, while also promoting gel formation in carbomer-based systems[27].

The final gel underwent gentle stirring to eliminate any entrapped air and was permitted to equilibrate. The formulated imiquimod topical gel underwent assessment for various physicochemical parameters, including appearance, pH, viscosity, spreadability, drug content uniformity, and in vitro drug release, to guarantee the quality and efficacy of the formulation. This approach produced a consistent, uniform, and user-friendly topical gel ideal for targeted dermatological use.

2.8 In-Vitro Release Study

The in-vitro release was conducted utilizing a synthetic membrane diffusion apparatus, sustained with phosphate buffered saline (pH 7.4) at a temperature of 37 ± 1°C. The formulation was introduced into the donor compartment, and the receptor phase was agitated at a speed of 100 rpm. Samples were collected at predetermined intervals, subjected to filtration, and subsequently analyzed using HPLC techniques. The kinetics of drug release were analyzed using mathematical models to elucidate the diffusion mechanism[28].

2.9 Cytotoxicity Study

Recent studies have extensively investigated the cytotoxicity of zinc oxide–loaded mesoporous silica nanoparticles (ZnO-MSNs) to establish their biosafety and therapeutic relevance. Assessments of cytotoxicity in vitro are routinely conducted on a variety of cell lines, including normal and disease-relevant types such as HaCaT keratinocytes, L929 or NIH-3T3 fibroblasts, HEK293 cells, and cancer cell lines like PC3, HeLa, or A431, to determine selectivity. Common colorimetric assays like MTT, WST-1, or CCK-8 are frequently utilized after 24–48 hours of exposure to different concentrations of ZnO-MSNs. In contrast to plain MSNs, the addition of ZnO typically leads to a decrease in cell viability that is both concentration- and time-dependent, which can be linked to the bioactive properties of ZnO. Numerous studies indicate that when ZnO is loaded at optimal levels, ZnO-MSNs exhibit excellent cytocompatibility (>80–90% cell viability) with normal cells, while also showing improved antiproliferative effects on diseased cells[29].

Investigations into the mechanisms indicate that the cytotoxic effects linked to ZnO-MSNs mainly stem from the generation of reactive oxygen species (ROS) and the release of Zn^{2+} ions, especially in acidic intracellular environments. Following cellular uptake through endocytosis, ZnO disintegrates within endolysosomal compartments, resulting in oxidative stress, mitochondrial impairment, and ultimately, apoptosis. This mechanism has undergone validation through various complementary assays, including intracellular ROS quantification via DCFH-DA, analysis of mitochondrial membrane potential using JC-1, and investigations into apoptosis and necrosis through Annexin V/PI staining and caspase-3 activation. Significantly, mesoporous silica serves as a protective and modulatory carrier, mitigating the burst toxicity typically linked to free ZnO nanoparticles and facilitating controlled intracellular Zn^{2+} release.

The evaluation of cytotoxicity was conducted using B16-F10 melanoma cells to assess the biological safety of both pure Imiquimod and its formulation. Cells underwent treatment with escalating concentrations of both samples, and cell viability was assessed utilizing an appropriate colorimetric assay. The half-maximal inhibitory concentration (IC_{50}) was determined, indicating a decrease in cytotoxicity for the ZnO-MSN formulation attributed to its controlled release properties[30].

3 RESULTS

3.1 Physical Characterization of Plain MSNs and ZnO-MSNs

The synthesized MCM-41 mesoporous silica nanoparticles demonstrated a consistent and clearly defined morphology along with a narrow particle size distribution, reflecting the successful development of an ordered mesoporous structure. The structural uniformity observed is characteristic of MCM-41 type materials, affirming the formation of a highly porous framework. This feature is especially beneficial for the effective loading and entrapment of poorly soluble therapeutic agents, including imiquimod. The uniformity in particle size and morphology indicates a reliable synthesis process, highlighting the nanoparticles' potential for use in pharmaceutical applications[31].

After the surface was functionalized with zinc oxide, a slight increase in the average particle size was noted. This change can be linked to the deposition or anchoring of ZnO moieties on the surface and within the pore openings of the silica framework. The plain MSNs displayed a particle size range of approximately 120-150 nm, whereas the ZnO-functionalized MSNs exhibited a larger size, falling within the range of 160-200 nm. The controlled size augmentation presents notable benefits, as the modification of ZnO enhances surface reactivity and boosts the carrier system's affinity for imiquimod. Furthermore, the inclusion of ZnO is anticipated to enhance therapeutic compatibility and functionality, especially for topical applications, due to its established antimicrobial and bioactive characteristics[32].

The effective integration of zinc oxide within the mesoporous silica matrix was additionally validated by energy-dispersive X-ray spectroscopy (EDS) analysis. The elemental spectra displayed distinctive peaks associated with silicon (Si) and oxygen (O), aligning with the silica backbone, as well as unique zinc (Zn) signals in the ZnO-MSN formulation. The presence of these elements clearly confirms the successful functionalization of ZnO on the MSNs, reinforcing the structural and compositional integrity of the developed nanocarrier system[33].

3.2 Drug Loading and Entrapment Efficiency

The assessment of drug loading and entrapment efficiency is essential for understanding the performance of mesoporous silica nanoparticle-based drug delivery systems, as these factors directly impact dosage accuracy, release behavior, and therapeutic efficacy. The well-organized pore structure, substantial specific surface area, and adjustable pore size of mesoporous silica nanoparticles (MSNs), especially MCM-41 type materials, render them outstanding carriers for encapsulating poorly water-soluble drugs like imiquimod. Drug loading is typically accomplished using adsorption or solvent impregnation methods, where the drug permeates the mesoporous channels and is held in place through physical adsorption, hydrogen bonding, or electrostatic interactions with the silica surface [34].

Achieving high drug loading and entrapment efficiency is essential for topical formulations, as these factors contribute to minimizing the amount of carrier needed, enhancing drug stability, and ensuring prolonged drug release at the application site. Furthermore, effective entrapment reduces initial burst release and improves controlled diffusion from the mesoporous matrix. The integration of mesoporous silica architecture with zinc oxide surface functionalization establishes a strong foundation for attaining high drug loading capacity and optimal entrapment efficiency, thus facilitating the advancement of effective and patient-friendly topical nanocarrier systems.

Drug loading efficiency significantly improved after ZnO functionalization. This enhancement may be attributed to increased surface-active sites provided by ZnO, allowing stronger interaction between Imiquimod and the carrier matrix. Compared to plain MSNs, ZnO-functionalized MSNs demonstrated a notably higher entrapment efficiency and drug loading capacity. The **Table 3** clearly states the difference between plain MSNs and Zinc oxide loaded MSNs. The improved entrapment suggests that ZnO functionalization enhances drug affinity and protects the drug within the porous structure, enabling a more controlled and sustained release.

Table 3 Comparative %EE and %LC of MSNs vs. ZnO-MSNs

Parameter	Plain MSNs	ZnO-MSNs
% Entrapment Efficiency	~45–55%	~65–75%
% Loading Capacity	~10–15%	~20–25%

3.3 *In-Vitro* Drug Release

The **Table 4** mentions the *In-vitro* drug release studies that were conducted utilizing a synthetic membrane diffusion apparatus to assess the release characteristics of the formulation under regulated conditions upto 72 hours. A properly prepared synthetic membrane, which had been immersed in

phosphate-buffered saline (PBS), was positioned between the donor and receptor compartments of the diffusion apparatus. The receptor compartment was filled with phosphate-buffered saline (pH 7.4), serving as the release medium to simulate physiological conditions. The system was maintained at a constant temperature of 37 ± 1 °C using a thermostatically controlled water bath to mimic in vivo skin temperature[35].

A specific amount of the formulation was precisely positioned in the donor compartment, guaranteeing consistent interaction with the membrane surface. The receptor phase was kept in constant agitation at 100 rpm with a magnetic stirrer to uphold sink conditions and guarantee an even distribution of the released drug across the medium. At predetermined time intervals, aliquots of the receptor medium were withdrawn carefully and immediately replaced with an equal volume of fresh PBS maintained at the same temperature to preserve constant volume and sink conditions. The gathered samples underwent filtration using an appropriate membrane filter to eliminate any particulate matter before analysis[36].

The samples that were filtered underwent quantitative analysis through a validated high-performance liquid chromatography (HPLC) method to ascertain the total amount of drug released over time. The release data were presented as cumulative percentage of drug release over time. Additionally, the release profiles obtained were analyzed using several mathematical kinetic models, such as zero-order, first-order, Higuchi, and Korsmeyer–Peppas models, to clarify the drug release kinetics and identify the primary mechanism driving drug diffusion from the formulation[37].

Table 4 Release profile of Imiquimod loaded ZnO-MSN gel

Time (Hrs)	Imiquimod loaded ZnO-MSNs Containing Gel
0	0
10 min	0
30 min	2.76 ±2.64
1	4.86± 2.15
2	9.13 ± 1.98
4	13.96 ± 2.19
8	24.73 ± 1.83
12	32.12 ± 1.45
24	46.39 ± 1.59
48	57.35 ± 1.14
60	67.26 ± 1.38
72	74.68 ±1.87

The diffusion study showed a biphasic release pattern, with an initial burst followed by prolonged drug release. ZnO-MSN gel exhibited a controlled release (~60–70%), reducing sudden exposure and potential inflammatory responses. The release kinetics best fitted the Higuchi diffusion model, confirming that drug transport occurs via diffusion through a porous matrix rather than rapid dissolution. The **Table 5** displays the linear regression coefficients (R^2 values) derived from fitting the in-vitro drug release data of the imiquimod-loaded ZnO-MSN-containing gel to a range of mathematical kinetic models. These models are frequently employed to clarify the mechanisms that regulate drug release from controlled delivery systems [38].

The zero-order model demonstrated a R^2 value of 0.8276, suggesting a less satisfactory fit in comparison to alternative models. This indicates that the release of the drug from the formulation is not happening at a steady rate that is unaffected by drug concentration, which aligns with expectations for matrix-based nanoparticulate gels. In a similar vein, the first-order model demonstrated a moderate correlation coefficient ($R^2 = 0.8923$), suggesting that drug release is somewhat influenced by concentration, though it is not the primary mechanism governing the release process[39].

The Korsmeyer–Peppas model exhibited the highest linear regression coefficient ($R^2 = 0.9777$), signifying it as the most suitable fit among the models evaluated. The findings indicate that the release of imiquimod from the ZnO-MSN gel is likely governed by a diffusion-controlled mechanism, potentially involving anomalous (non-Fickian) transport. This behavior may stem from the interplay between drug diffusion through the mesoporous silica network and the relaxation of the polymer within the gel matrix. The excellent alignment with this model underscores the intricate release dynamics influenced by the nanocarrier system alongside the gel base[40].

The Higuchi model demonstrated a strong correlation ($R^2 = 0.9435$), reinforcing the notion that diffusion plays a significant role in the drug release from the formulation. Conversely, the Hixson–Crowell model demonstrated a lower R^2 value of 0.8717, suggesting that variations in surface area and particle erosion have a limited impact on the release process. The release kinetics of the imiquimod-loaded ZnO-MSN gel are most accurately characterized by the Korsmeyer–Peppas model, highlighting a notable influence from diffusion-controlled mechanisms. This

supports the formulation's capacity for delivering controlled and sustained drug release, making it appropriate for topical therapeutic applications[41].

Table 5 Kinetic model comparison for Imiquimod loaded ZnO-MSNs

Formulation	Linear Regression Coefficient (R^2)				
	Zero Order Model	First Order Model	Korsemeyer-Peppas Model	Hixson-Crowell Model	Higuchi Model
Imiquimod loaded ZnO-MSNs Containing Gel	0.8276	0.8923	0.9777	0.8717	0.9435

3.4 Cytotoxicity Study

Cytotoxicity studies using B16-F10 melanoma cells revealed a marked difference between the free drug and the formulation. Free Imiquimod showed strong cytotoxicity with a lower IC_{50} value (~7.3 µg/mL), indicating higher irritation potential. In contrast, the ZnO-MSN formulation exhibited a higher IC_{50} (~11.7 µg/mL), demonstrating reduced cytotoxicity due to the protective and controlled release effect of the nanocarrier system. These results confirm that the formulation is less aggressive yet remains therapeutically effective.

The data on cell viability reveal a distinct concentration-dependent cytotoxic effect for both the free active pharmaceutical ingredient and the active pharmaceutical ingredient-loaded mesoporous silica nanoparticles. With the increase in concentration from 20 to 100 µg/mL, there is a noticeable decrease in percentage cell viability in both groups, suggesting a dose-dependent biological response. At every concentration tested, the formulation loaded with the API consistently demonstrates greater cell viability than the free API, underscoring a significant distinction in the cytotoxic profiles of the two systems.

At lower concentrations (20-40 µg/mL), the free API exhibits moderate cytotoxicity, with cell viability declining from around 85% to 70%. In contrast, the API-loaded MSNs sustain high cell viability, ranging from approximately 90% to 95%. This trend is increasingly evident at elevated concentrations, where exposure to free API results in a significant decrease in viability, dropping to approximately 48% and 42% at 80 and 100 µg/mL, respectively. Conversely, cells exposed to the API-loaded MSN formulation demonstrate markedly enhanced viability, maintaining approximately 75% at 80 µg/mL and around 65% even at the maximum concentration tested.

The **Figure 5** demonstrate that the incorporation of the active pharmaceutical ingredient within mesoporous silica nanoparticles markedly diminishes its cytotoxic effects on cellular structures. The enhanced compatibility of the API-loaded MSNs is due to their ability to release drugs in a controlled and sustained manner, thereby reducing the risk of abrupt high drug exposure and the consequent cellular stress. This protective effect highlights the potential benefits of MSN-based nanocarriers in improving the safety profile of powerful therapeutic agents.

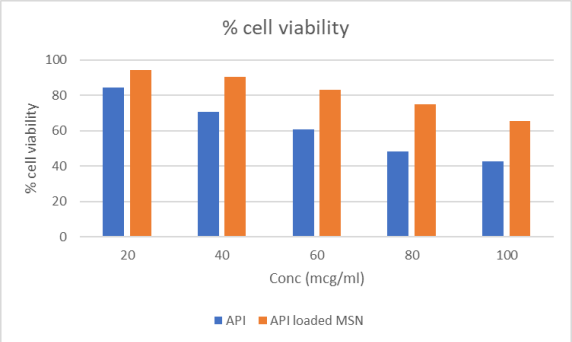

Figure 5 Cytotoxicity profile demonstrating reduced toxicity of ZnO-MSN formulation

4 DISCUSSION

The combination of zinc oxide and mesoporous silica nanoparticles yielded multiple synergistic benefits that together improved the efficacy of the formulated topical delivery system. The elevated surface area and meticulously structured pore architecture of MSNs enabled exceptional drug loading, while the incorporation of ZnO significantly enhanced drug–carrier interactions, leading to improved entrapment efficiency. The composite system demonstrated consistent and reliable drug release kinetics, effectively reducing burst release and allowing for extended therapeutic presence at the application site. The integration of the drug into the ZnO-MSN matrix notably diminished cytotoxicity and irritation potential in comparison to the free drug, which is an essential factor for long-term topical treatment.

Beyond its function as a carrier, ZnO also offers inherent properties that benefit the skin, such as anti-inflammatory effects, protection against UV radiation, and enhancement of wound healing, all of which are especially beneficial in the treatment of skin cancers. Moreover, the nanostructured ZnO-MSN system

demonstrated an ability to enhance drug retention within the targeted skin layers, which may lead to improved local efficacy and a reduction in systemic exposure. The findings collectively support the hypothesis that ZnO-MSNs serve as an advanced and logical delivery platform for topical imiquimod in the management of basal cell carcinoma, effectively overcoming significant limitations linked to traditional formulations, including poor tolerability, uncontrolled release, and inadequate dermal retention.

5 CONCLUSION

This study effectively showcases the design, development, and evaluation of imiquimod-loaded zinc oxide–functionalized mesoporous silica nanoparticles (ZnO-MSNs) as a sophisticated topical drug delivery system for managing basal cell carcinoma (BCC). The thoughtful combination of mesoporous silica nanoparticles with zinc oxide has led to the development of a multifunctional nanocarrier platform that effectively addresses various limitations found in traditional imiquimod formulations. The organized mesoporous architecture of MSNs facilitated substantial drug loading and effective entrapment of imiquimod, while the functionalization with ZnO significantly improved drug–carrier interactions and the stability of the formulation. The inclusion of zinc oxide provided various therapeutic benefits and enhancements related to the formulation. In addition to enhancing drug loading efficiency, ZnO played a role in minimizing irritation potential and improving biocompatibility, both of which are essential factors for sustained topical treatment. Furthermore, the natural advantages of ZnO for skin health such as its anti-inflammatory effects, UV shielding capabilities, and potential for promoting wound healing provide significant therapeutic benefits in addressing skin cancers like BCC, particularly when the skin barrier is frequently at risk. The gel formulation based on ZnO-MSN demonstrated a sustained and controlled release of the drug, effectively reducing the initial burst effect typically seen with topical imiquimod therapy. The observed controlled release behavior, along with a notable reduction in cytotoxicity relative to pure imiquimod, suggests enhanced tolerability and a more consistent therapeutic response at the target site. This adjustment in drug exposure is anticipated to improve patient adherence and minimize the adverse skin reactions commonly associated with current commercial formulations. The results of this study demonstrate that ZnO-functionalized MSNs represent a promising and patient-friendly nanocarrier system for the topical delivery of imiquimod in the treatment of basal cell carcinoma. The formulated approach enhances the efficiency and safety of drug delivery while effectively tackling the significant limitations associated with traditional therapies. This nanoplatform presents significant promise as a practical option for the management of topical BCC and deserves additional in vivo and clinical assessment to validate its potential for real-world application.

6 ACKNOWLEDGMENT

The author expresses sincere gratitude to RK University, Rajkot, for providing the necessary academic support and infrastructure to perform the research work.

7 CONFLICT OF INTEREST

The author declares no conflict of interest.

8 CREDIT AUTHOR CONTRIBUTION

Conceptualization: Samir Atara, Shubham Solanki; **Data Curation**: Shubham Solanki; **Formal Analysis**: Shubham Solanki, Samir Atara; **Writing-original draft**: Shubham Solanki, Mangesh Kulkarni; **Writing-review & editing**: Samir Atara, Shubham Solanki.

9 REFERENCES

- [1] Sergi MC, Ambrogio F, Della Mura M, Sorino J, Cazzato G. Basal Cell Carcinoma: An Old Friend with Multiple Faces. Cancers (Basel) 2025;17. https://doi.org/10.3390/cancers17060993.
- [2] Bichakjian C, Armstrong A, Baum C, Bordeaux JS, Brown M, Busam KJ, et al. Guidelines of care for the management of basal cell carcinoma. J Am Acad Dermatol 2018;78:540–59. https://doi.org/10.1016/J.JAAD.2017.10.006.
- [3] Anand P, Kunnumakara AB, Sundaram C, Harikumar KB, Tharakan ST, Lai OS, et al. Cancer is a preventable disease that requires major lifestyle changes. Pharm Res 2008;25:2097–116. https://doi.org/10.1007/S11095-008-9661-9.
- [4] Mucci LA, Wedren S, Tamimi RM, Trichopoulos D, Adami HO. The role of gene-environment interaction in the aetiology of human cancer: examples from cancers of the large bowel, lung and breast. J Intern Med 2001;249:477–93. https://doi.org/10.1046/J.1365-2796.2001.00839.X.

- [5] Asefa T, Tao Z. Mesoporous silica and organosilica materials — Review of their synthesis and organic functionalization. Https://DoiOrg/101139/V2012-094 2012;90:1015–31. https://doi.org/10.1139/V2012-094.
- [6] Baba PUF, Hassan A ul, Khurshid J, Wani AH. Basal Cell Carcinoma: Diagnosis, Management and Prevention. Journal of Molecular Pathology 2024;5:153–70. https://doi.org/10.3390/jmp5020010.
- [7] Mannino M, Scalvenzi M, Di Stefani A, Costa C, Calzavara-Pinton P, Fargnoli MC, et al. Clinical and Histological Predictors of Advanced Basal Cell Carcinoma Recurrence After Complete Response to Hedgehog Pathway Inhibitors: A Retrospective Multicenter Observational Study. Cancers (Basel) 2025;17. https://doi.org/10.3390/cancers17111840.
- [8] Jeelani PG, Mulay P, Venkat R, Ramalingam C. Multifaceted Application of Silica Nanoparticles. A Review. Silicon 2019 12:6 2019;12:1337–54. https://doi.org/10.1007/S12633-019-00229-Y.
- [9] Trzeciak K, Chotera-ouda A, Bak-sypien II, Potrzebowski MJ. Mesoporous Silica Particles as Drug Delivery Systems—The State of the Art in Loading Methods and the Recent Progress in Analytical Techniques for Monitoring These Processes. Pharmaceutics 2021, Vol 13, 2021;13. https://doi.org/10.3390/PHARMACEUTICS13070950.
- [10] González S. Should reflectance confocal microscopy be the gold standard for basal cell carcinoma diagnosis? Imaging Med 2013;5:299–301. https://doi.org/10.2217/iim.13.36.
- [11] Anjum S, Hashim M, Malik SA, Khan M, Lorenzo JM, Abbasi BH, et al. Recent Advances in Zinc Oxide Nanoparticles (ZnO NPs) for Cancer Diagnosis, Target Drug Delivery, and Treatment. Cancers (Basel) 2021;13:4570. https://doi.org/10.3390/CANCERS13184570.
- [12] Cao S, Chang J, Fang L, Wu L. Metal Nanoparticles Confined in the Nanospace of Double-Shelled Hollow Silica Spheres for Highly Efficient and Selective Catalysis. Chemistry of Materials 2016;28:5596–600. https://doi.org/10.1021/ACS.CHEMMATER.6B02209.
- [13] Jang KS, Kim HJ, Johnson JR, Kim WG, Koros WJ, Jones CW, et al. Modified Mesoporous Silica Gas Separation Membranes on Polymeric Hollow Fibers. Chemistry of Materials 2011;23:3025–8. https://doi.org/10.1021/CM200939D.
- [14] Chen D, Li N, Tang F, Qi S. Facile and scalable synthesis of tailored silica “nanorattle” structures. Advanced Materials 2009;21:3804–7. https://doi.org/10.1002/ADMA.200900599;REQUESTEDJOURNAL:JOURNAL:15214095;WGROUP:STRING:PUBLICATION.
- [15] Teng Z, Han Y, Li J, Yan F, Yang W. Preparation of hollow mesoporous silica spheres by a sol–gel/emulsion approach. Microporous and Mesoporous Materials 2010;127:67–72. https://doi.org/10.1016/J.MICROMESO.2009.06.028.
- [16] Ashour MM, Mabrouk M, Soliman IE, Beherei HH, Tohamy KM. Mesoporous silica nanoparticles prepared by different methods for biomedical applications: Comparative study. IET Nanobiotechnol 2021;15:291. https://doi.org/10.1049/NBT2.12023.
- [17] Vazquez NI, Gonzalez Z, Ferrari B, Castro Y. Synthesis of mesoporous silica nanoparticles by sol–gel as nanocontainer for future drug delivery applications. Boletín de La Sociedad Española de Cerámica y Vidrio 2017;56:139–45. https://doi.org/10.1016/J.BSECV.2017.03.002.
- [18] Shen Z, Zhou H, Chen H, Xu H, Feng C, Zhou X. Synthesis of Nano-Zinc Oxide Loaded on Mesoporous Silica by Coordination Effect and Its Photocatalytic Degradation Property of Methyl Orange. Nanomaterials 2018;8:317. https://doi.org/10.3390/NANO8050317.
- [19] Mihai GD, Meynen V, Mertens M, Bilba N, Cool P, Vansant EF. ZnO nanoparticles supported on mesoporous MCM-41 and SBA-15: a comparative physicochemical and photocatalytic study. Journal of Materials Science 2010 45:21 2010;45:5786–94. https://doi.org/10.1007/S10853-010-4652-8.
- [20] Vagena IA, Gatou MA, Theocharous G, Pantelis P, Gazouli M, Pippa N, et al. Functionalized ZnO-Based Nanocomposites for Diverse Biological Applications: Current Trends and Future

Perspectives. Nanomaterials 2024, Vol 14, 2024;14. https://doi.org/10.3390/NANO14050397.

- [21] Sathe P, Saka R, Kommineni N, Raza K, Khan W. Dithranol-loaded nanostructured lipid carrier-based gel ameliorate psoriasis in imiquimod-induced mice psoriatic plaque model. Drug Dev Ind Pharm 2019;45:826–38. https://doi.org/10.1080/03639045.2019.1576722;SUBPAGE:STRING:ACCESS.
- [22] Rahangdale M, Solanki S, Patil P, Bhavsar D, Sawant K. Fabrication and characterization of apremilast-loaded zinc oxide-mesoporous silica nanoparticles for psoriasis treatment. Ther Deliv 2024;15:449. https://doi.org/10.1080/20415990.2024.2343646.
- [23] Kim S, Abdella S, Abid F, Afinjuomo F, Youssef SH, Holmes A, et al. Development and Optimization of Imiquimod-Loaded Nanostructured Lipid Carriers Using a Hybrid Design of Experiments Approach. Int J Nanomedicine 2023;18:1007. https://doi.org/10.2147/IJN.S400610.
- [24] Formulation and Evaluation of Imiquimod Loaded Nanosuspension Gel for Transdermal Delivery 2020.
- [25] Jadhav ST, Salunkhe VR, Bhinge SD, Honmane SM, Jadhav AS. Development and evaluation of imiquimod-loaded nanoemulsion-based gel for the treatment of skin cancer. Future Journal of Pharmaceutical Sciences 2024 10:1 2024;10:93-. https://doi.org/10.1186/S43094-024-00660-Y.
- [26] da Silva EL, Pedraça ES, Salgueiro AP, Gazzi RP, Nunes JS, Cavagni J, et al. Efficacy and safety of a 0.05 % nanoencapsulated imiquimod hydrogel for the treatment of actinic cheilitis: Drug release analysis and clinical study. Nanomedicine 2024;62:102779. https://doi.org/10.1016/J.NANO.2024.102779.
- [27] Maocha I, Rosado B, Lopes-Nunes J, Lopes M, Rolo J, Pires B, et al. Imiquimod-Loaded Nanosystem for Treatment Human Papillomavirus-Induced Lesions. Pharmaceutics 2024;16. https://doi.org/10.3390/PHARMACEUTICS16070864/S1.
- [28] Anas Al Tahan M, Marwah M, El-Zein H, Al Tahan S, Sanchez-Aranguren L. Exploring mesoporous silica microparticles in pharmaceutical sciences: Drug delivery and therapeutic insights. Int J Pharm 2025;678:125656. https://doi.org/10.1016/J.IJPHARM.2025.125656.
- [29] Li J, Chen H, Rui Q, Liu P, Cai W, Kong Y, et al. Biodegradable Controlled Drug Delivery Platform Based on Carboxylated Mesoporous Silica Nanoparticles—Zinc Oxide Quantum Dots. Ind Eng Chem Res 2024;63:13459–68. https://doi.org/10.1021/ACS.IECR.4C01115.
- [30] Karnopp JCF, Jorge J, da Silva JR, Boldo D, Del Pino Santos KF, Duarte AP, et al. Synthesis, Characterization, and Cytotoxicity Evaluation of Chlorambucil-Functionalized Mesoporous Silica Nanoparticles. Pharmaceutics 2024;16. https://doi.org/10.3390/PHARMACEUTICS16081086/S1.
- [31] Majidi RF, Mesgar ASM, Milan PB. Surface-modified, zinc-incorporated mesoporous silica nanoparticles with improved antibacterial and rapid hemostatic properties. Colloids Surf B Biointerfaces 2024;243:114132. https://doi.org/10.1016/J.COLSURFB.2024.114132.
- [32] Almatroudi A, Almatroudi A. Advances in Mesoporous Silica and Hybrid Nanoparticles for Drug Delivery: Synthesis, Functionalization, and Biomedical Applications. Pharmaceutics 2025, Vol 17, 2025;17. https://doi.org/10.3390/PHARMACEUTICS17121602.
- [33] Fotie J, Fotie J. Applications of Tailored Mesoporous Silicate Nanomaterials in Regenerative Medicine and Theranostics. International Journal of Molecular Sciences 2025, Vol 26, 2025;26. https://doi.org/10.3390/IJMS26167918.
- [34] Zhou Y, Quan G, Wu Q, Zhang X, Niu B, Wu B, et al. Mesoporous silica nanoparticles for drug and gene delivery. Acta Pharm Sin B 2018;8:165. https://doi.org/10.1016/J.APSB.2018.01.007.
- [35] Al Tahan MA, Al Tahan S. Pioneering Advances and Innovative Applications of Mesoporous Carriers for Mitochondria-Targeted Therapeutics. Br J Biomed Sci 2024;81:13707.

https://doi.org/10.3389/BJBS.2024.13707/FULL.

- [36] Li M, Sun J, Zhao D, Zhang W, Xu Q. Inhibitory impact of a mesoporous silica nanoparticle-based drug delivery system on Porphyromonas gingivalis-induced bone resorption. Journal of Materials Science: Materials in Medicine 2024 35:1 2024;35:56-. https://doi.org/10.1007/S10856-024-06827-6.
- [37] Khalbas AH, Albayati TM, Ali NS, Salih IK. Drug loading methods and kinetic release models using of mesoporous silica nanoparticles as a drug delivery system: A review. S Afr J Chem Eng 2024;50:261–80. https://doi.org/10.1016/J.SAJCE.2024.08.013.
- [38] Khalbas AH, Albayati TM, Ali NS, Salih IK. Drug loading methods and kinetic release models using of mesoporous silica nanoparticles as a drug delivery system: A review. S Afr J Chem Eng 2024;50:261–80. https://doi.org/10.1016/J.SAJCE.2024.08.013.
- [39] Zhu W, Long J, Shi M. Release Kinetics Model Fitting of Drugs with Different Structures from Viscose Fabric. Materials 2023, Vol 16, 2023;16. https://doi.org/10.3390/MA16083282.
- [40] Galdopórpora JM, Olivera MV, Ibar A, Farriol DH, Desimone MF, Queirolo CMM, et al. Controlled release of dexamethasone phosphate from modified mesoporous biocompatible silica nanoparticles: synthesis, characterization, and kinetic studies. Open Exploration 2019 3: 2025;3:100895-. https://doi.org/10.37349/EDS.2025.100895.
- [41] Shahein SA, Aboul-Enein AM, Higazy IM, Abou-Elella F, Lojkowski W, Ahmed ER, et al. Targeted anticancer potential against glioma cells of thymoquinone delivered by mesoporous silica core-shell nanoformulations with pH-dependent release. Int J Nanomedicine 2019;14:5503. https://doi.org/10.2147/IJN.S206899